

# SOAR BVI Photometry of the Metal-poor Bulge Globular Cluster NGC 6642 <sup>★</sup>

B. Barbuy<sup>1</sup>, E. Bica<sup>2</sup>, S. Ortolani<sup>3</sup>, and C. Bonatto<sup>2</sup>

<sup>1</sup> Universidade de São Paulo, Dept. de Astronomia, Rua do Matão 1226, São Paulo 05508-090, Brazil

email: barbuy@astro.iag.usp.br

<sup>2</sup> Universidade Federal do Rio Grande do Sul, Dept. de Astronomia, CP 15051, Porto Alegre 91501-970, Brazil

email: bica@if.ufrgs.br

<sup>3</sup> Università di Padova, Dipartimento di Astronomia, Vicolo dell'Osservatorio 2, I-35122 Padova, Italy

email: ortolani@pd.astro.it

Received ; accepted

**Abstract.** We present BVI photometry of the globular cluster NGC 6642 using the SOI imager at the SOAR Telescope. The Colour Magnitude Diagrams (CMD) reach  $\approx 1.5$  mag in V below the main sequence turn-off. A comparison of the overall sequences, and in particular the Red Giant Branch slope of NGC 6642 with that of M5 indicates that the two clusters must have a similar metallicity of  $[\text{Fe}/\text{H}] \approx -1.3$ . We also obtain for NGC 6642 a reddening  $E(\text{B}-\text{V})=0.42\pm 0.03$ , and a distance from the Sun of  $d_{\odot}=7.2\pm 0.5$  kpc. Therefore NGC 6642 is a moderately metal-poor globular cluster, spatially located in the bulge, at a galactocentric distance of  $R_{\text{GC}} \approx 1.7$  kpc. The comparison of CMDs of NGC 6642 with those of M5 shows that there is a very good match of magnitude difference between turn-off and horizontal branch, suggesting comparable ages. M5 has an age typical of the halo globulars, and consequently NGC 6642 is coeval with the halo. NGC 6642 is a good candidate to be one of the few genuine metal-poor and old *bulge* clusters, and might be one of the most ancient fossils in the Galaxy.

**Key words.** The Galaxy: Globular Clusters: NGC 6642 – HR diagram

## 1. Introduction

For the vast majority of the known globular clusters in the Galaxy (Harris 1996, as updated at <http://www.physics.mcmaster.ca/Globular.html>), the properties have already been inferred by means of Colour-Magnitude Diagrams (CMD). Until recently, no optical CMD was available for NGC 6642. In Barbuy et al. (1999) a revision of clusters within  $20^\circ \times 20^\circ$  around the Galactic center was presented, where NGC 6642 was not included due at the time to a lack of information on its HB morphology and distance to the Galactic center.

In Piotto et al. (2002), 74 CMDs in the HST WFPC2 F439W and F555W bands were presented. NGC 6642 is included in that study, however reddening and distance were adopted from Harris (1996). A JK CMD was presented by Minniti, Olszewski, & Rieke (1995), who detected the cluster's Red Giant Branch (RGB). Recio-Blanco et al. (2005) using Hubble data derived  $E(B - V) = 0.44$  and an apparent distance modulus  $(m - M)_{F555W} = 16.70$ .

NGC 6642, also designated ESO 522-SC32 and GCL 97, is located at  $\alpha_{2000} = 18^{\text{h}} 31^{\text{m}} 54.3^{\text{s}}$ ,  $\delta_{2000} = -23^\circ 28' 35''$  ( $\ell = 9.81^\circ$ ,  $b = -6.44^\circ$ ). It is in Sagittarius, projected not far from the Galactic center. Trager et al (1995) estimated a core radius  $R_{\text{core}} = 6.2''$ , a concentration parameter  $c = 1.99$ , which imply a tidal radius  $r_t \approx 10'$ . The half-light radius is  $r_h = 44''$ . Minniti (1995) derived  $[\text{Fe}/\text{H}] = -1.40$  from the spectroscopy of 13 individual cluster stars. The compilation by Harris (1996) provides  $[\text{Fe}/\text{H}] = -1.35$ ,  $E(B - V) = 0.41$ ,  $d_\odot = 7.7$  kpc.

In such central direction, bulge and inner halo are superimposed, and it is important to derive accurate positions, kinematical data, metallicity and abundance ratios to characterize membership of globular clusters with respect to both Galactic subsystems. Previous data indicate that NGC 6642 is a metal-poor globular cluster located in the bulge, and such borderline objects may provide clues on the bulge/inner halo issue, and in turn, on the early stages of the Galactic bulge formation.

In this work we present deep BVI CMDs for NGC 6642, deriving reddening, metallicity and distance. We also determine the age, for the first time for this cluster.

In Section 2 we describe the observations, data reduction and calibration procedures. In Section 3 we present the CMDs and measure cluster parameters. In Section 4 the relative age of NGC 6642 is derived and discussed. Concluding remarks are given in Section 5.

## 2. Observations

The SOAR is a 4.1m telescope, located at Cerro Pachon, Chile, and operated by AURA, for the consortium composed by CNPq-Brazil, NOAO, UNC and MSU.

---

\* Observations collected with the SOAR Telescope, at Cerro Pachon, Chile

**Table 1.** *Log of observations.*

Target	Filter	Seeing (")	Exp.Time [s]	date
NGC 6642	B	0.9x0.8	15	06.06.2005
	B		15	"
	B		15	"
	B		15	"
	B	1.1x0.9	1080	"
	B	0.9x0.8	15	10.07.2005
	B	"	"	"
	B	"	"	"
	B	"	"	"
	B	"	"	"
	I	0.9x0.7	5	"
	I	0.78x0.75	"	"
	I	0.8x0.75	"	"
	I	0.8x0.7	"	"
	I	0.8x0.7	"	"
	V	0.8x0.7	7	"
	V	0.8x0.7	"	"
	V	0.9x0.9	"	"
	V	1.0x0.9	"	"
V	0.8x0.75	600	"	
V	0.9x0.8	"	"	
V	1.0x0.9	"	"	
I	0.9x0.8	420	26.07.2005	

SOAR is presently being commissioned for the first time to scientific use. The SOAR Optical Imager (SOI) is a bent-Cassegrain mounted optical imager using two EEV 2050 × 4100 CCDs, to cover a 5.26 arcminute square field of view at a scale of 0.077"/pixel.

The observations of NGC 6642 were carried out by the SOAR staff in June and July 2005 (Table 1) with the SOAR SOI camera in the B, V and I bands. The full image has a gap of 10.8" between the 2 CCDs. A binning 2 × 2 results in a pixel size of 0.154".

The images were flatfielded, bias subtracted, trimmed, and mosaiced by the SOAR Staff members. The photometry was carried out using the DAOPHOT and ALLSTAR codes (Stetson 1994).

The absolute calibration was obtained from the standard stars in the region Markarian A (Landolt 1992) observed on July 10th. This field is projected quite close to the cluster on the sky and it contains standards spanning a wide range in colour ( $-0.24 < V - I < 1.1$ ). The standard fields have been observed several times in BVI, collecting a total of 18

standard frames, almost all at the same airmass (1.19 - 1.21) in the night of July 10th. All the standard star images have been measured with MIDAS codes, using an aperture of 50 pixels, considerably larger than the seeing of FWHM (5-6 pixels), in order to avoid effects of frame to frame seeing variations. The very small instrumental magnitude variations of the same standards in different frames ( $< 0.01$  mag.) indicate that the night was photometric. The calibration equations, transforming the instrumental magnitudes ( $bvi$ ) into calibrated magnitudes (BVI) obtained from these standards are:

$$V = v - 0.08(V - I) + 28.60$$

$$I = i + 0.03(V - I) + 27.77$$

$$B = b + 0.03(B - V) + 29.19$$

$$V = v - 0.09(B - V) + 28.60$$

for 15s in  $V$ , 10s in  $I$  and 25s in  $B$  at 1.2 airmasses. The zero point errors in the equations are about 0.01 mag. The first set of observations (June 6th) and the long exposure I image obtained on July 26th have been calibrated using the July 10th calibration, by transfer of 8 bright and isolated stars in common. Calibration of red stars is a well known problem because of lack of high quality, very red standards. Stars redder than  $V - I \approx 1.0 - 1.2$  are not only statistically rare, but often are long period variables, and only in a few cases they are heavily reddened normal stars (F-G type). When available, these stars often show a wide scatter about the linear extrapolation of the calibration from bluer stars. In this case we prefer to use the extrapolation. In the present case, as usually occurs with CCD photometric systems, the colour terms are rather small and, consequently the calibrations do not depart much from the linear extrapolations, indicating that the passband system matches well the standard Johnson-Cousins system adopted in the Landolt standards. We also checked the colour term calibration using our previous observations obtained at the ESO Danish 1.5m telescope in 2000, calibrated using Landolt (1992) standard stars from the T Phoenix field containing standards with  $V - I \leq 1.65$ . No significant colour deviation was detected.

The photometric errors in NGC 6642 photometry can be obtained directly from DAOPHOT-Allstars outputs. The program gives the poissonian noise from the sky and star counts. The errors are less than 0.01 mag between  $V=13$  and 16, and reach 0.015 at  $V=17.5$  in the short exposure  $V$  frames (7s).

In the case of crowded fields such as in NGC 6642, however, the poissonian noise is a lower limit indication of the real photometric error because it increases only as a consequence of the higher background level. It does not take into account the spatial noise (the residual noise from the flat fielding) neither the fitting errors induced by the blends. Extensive tests carried out in the past demonstrated that the poissonian errors in globular cluster crowded fields are typically 3-4 time lower than the errors derived from frame to frame or from artificial star experiments. For this reason we independently evaluated the photometric errors in the cluster area from frame to frame comparisons.

**Table 2.** *Variable stars in the direction of NGC 6642.*

Variable	$V$	$B - V$	notes
V1	13.1	2.1	long period
V2	16.3	1.2	type non-identified
V3	16.3	0.6	RR Lyrae
V4	16.6	0.7	"
V5	16.7	0.8	"
V7	16.5	0.6	"
V9	16.4	0.8	"
V11	16.2	0.8	"
V12	16.2	0.7	"
V13	16.6	0.8	"
V15	16.3	0.6	"

Using  $V$  images with exposure times of 7s and 600s, errors of 0.015 mag have been derived at  $V=15$ , increasing up to 0.07 mag at  $V=18$ , close to the limiting magnitude of the short exposure frame. In principle these numbers should be representative of errors in the short exposures because the signal to noise in the long exposure is considerably higher. A realistic evaluation of the photometric errors in crowded fields affected by differential reddening, is difficult to measure. Still the frame to frame method does not fully take into account the blends because, if the seeing is not very different in the two frames, the blend effects are similar, but it takes into account the spatial noise and residual defects of the detector (important mainly for bright stars) because the images are shifted by several pixels. This means that the frame to frame errors, while more realistic of the poissonian error alone, still give a somewhat lower limit.

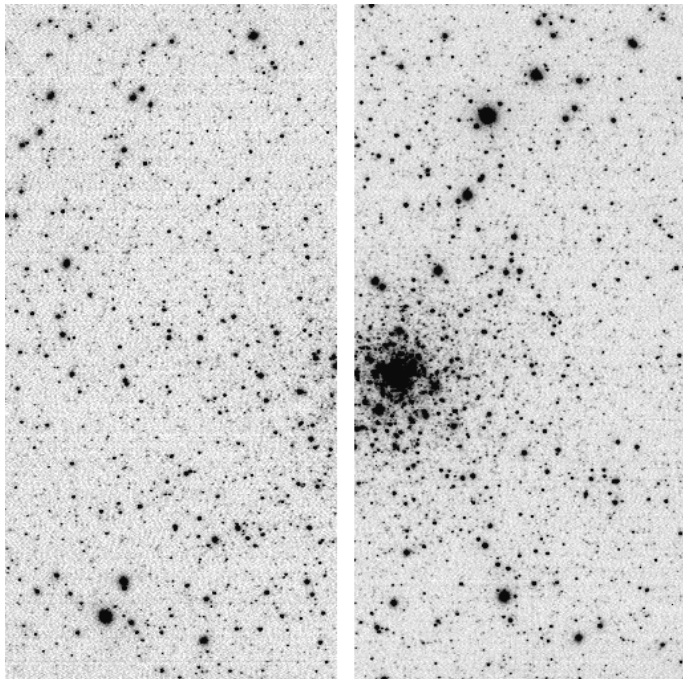
In the subsequent analyses, we will employ CMDs derived from the combination of the short and long exposures, in order to avoid saturation effects.

Fig. 1 shows a 7 sec.  $V$  image of NGC 6642.

### 3. Colour-Magnitude Diagrams

Figs. 2a,b show full field CMDs in  $V$  vs.  $B - V$  and  $V$  vs.  $V - I$ . The horizontal branch (HB) is relatively rich in stars and well defined. The HB morphology includes blue and red stars with respect to the RR-Lyrae gap. Some Asymptotic Giant Branch (AGB) stars are also present.

After trying to fit the mean loci of a number of template clusters of different metallicities to the CMD of NGC 6642, we found that the best match is obtained using the CMD of M5 (NGC 5904), after applying the appropriate shifts in magnitude and colour. In Fig. 3 we show the  $V$  vs.  $B - V$  CMD for an extraction of  $0.13' < R < 1.3'$ , where the

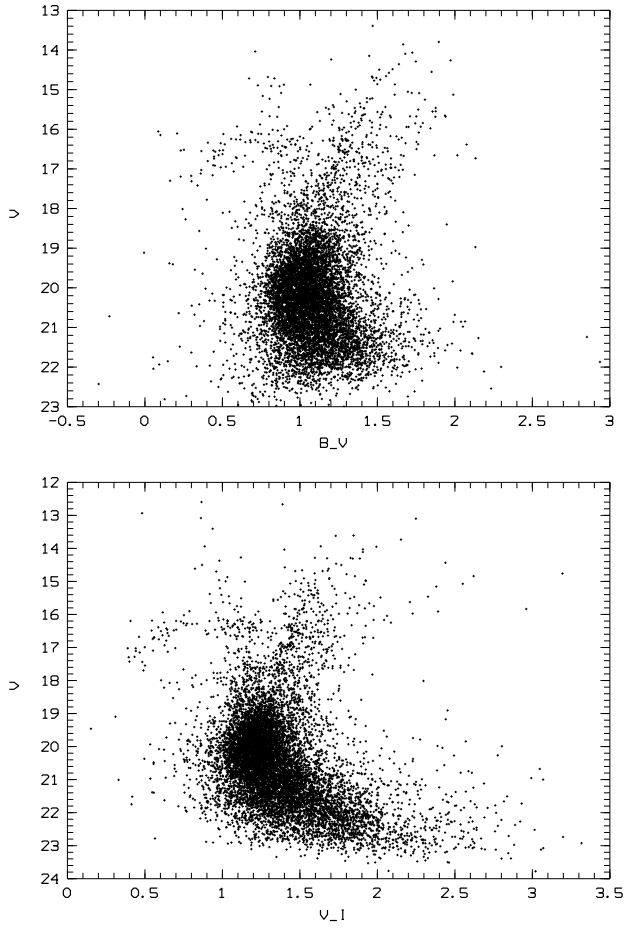


**Fig. 1.** NGC 6642 7 sec.  $V$  image. Dimensions are  $5.26' \times 5.26'$ . North is up and East is to the left.

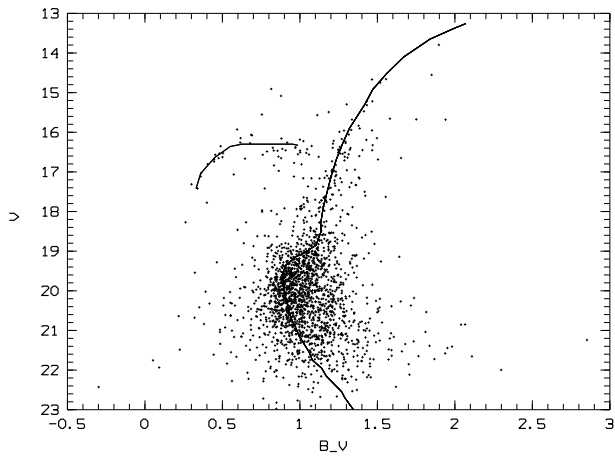
mean locus of M5 from Johnson & Bolte (1998) is overplotted. The CMDs reach  $V \approx 21$  or almost  $\approx 1.5$  mag below the turn-off, which is located at  $V \sim 19.7$ .

Fig. 3 shows that the upper evolutionary sequences (RGB, SGB and HB) of NGC 6642 and M5 are essentially coincident (after applying shifts in magnitude of  $\Delta V=1.28$  and colour  $\Delta(B-V)=0.44$ , see below): in particular, the two RGBs have the same slope. Harris (1996) quotes a metallicity  $[Fe/H] = -1.29$  for M5. The good match shown in Figure 3 indicates that NGC 6642 must have  $[Fe/H] \approx -1.3$ , confirming the previous results of Minniti (1995).

The HB level is located at  $V_{HB} = 16.35 \pm 0.04$  if we take the blue and red sides of the HB variable gap. The average value of the  $V$  magnitudes of the 9 RR Lyrae we identified from Hazen (1993, hereafter H93) is  $V_{RR} = 16.43 \pm 0.06$ . It is not surprising that the average RR Lyrae magnitude is fainter because our measurements are from very short exposure times as compared to the RR Lyrae periods. Since the RR Lyrae have asymmetric light curves, with more time spent at fainter magnitudes we expect their instantaneous luminosities to vary from a minimum of 0.02 up to about 0.1 mag. fainter than the non variable HB stars. The colour of the giant branch at the level of the HB is  $B - V_{RGB}=1.26$  and  $V - I_{RGB}=1.46$ . For the reference cluster M5, the colours are  $B - V_{RGB} = 0.85$  (Sandquist et al. 1996), and  $V - I_{RGB} = 0.97$  (Johnson & Bolte 1998). Therefore  $\Delta(B-V)=1.26-0.85=0.41$  and  $\Delta(V-I)=1.46-0.97=0.51$ . Given that the M5 reddening is  $E(B-V)=0.03$  (Harris 1996) or  $E(V-I)=0.04$ , we have a reddening of  $E(B-V)=0.44$  and  $E(V-I)=0.54$  for NGC 6642. The latter gives  $E(B-V)=0.54/1.33=0.41$  using



**Fig. 2.**  $V$  vs.  $B - V$  and  $V$  vs.  $V - I$  full field CMDs of NGC 6642.



**Fig. 3.**  $V$  vs.  $B - V$  CMD of NGC 6642, for an extraction of  $0.13 \leq r(′) \leq 1.3$ . Mean locus of M5 CMD is overplotted, with shifts of  $\Delta V=1.28$  and  $\Delta(B-V)=0.44$ .

Dean, Warren & Cousins (1978). The small difference in the reddening obtained from the two colours is likely due to differences in the zero points of the photometries. Adopting an average of  $0.42 \pm 0.03$  and the total to selective absorption parameter  $R_V=3.1$  we get  $A_V = 1.30 \pm 0.09$ . The absolute distance modulus is  $(m-M)_0=16.35-1.30-0.74=14.3$  (where the

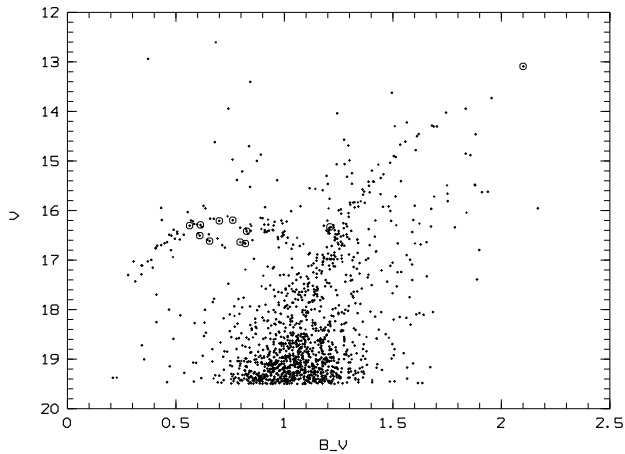


**Fig. 4.**  $V$  vs.  $B - V$  CMD of NGC 6642 where variables are indicated. Extraction is for  $r(') \leq 1.9$ .

$M_V=0.74$  has been adopted from Buonanno et al. 1989). Distance errors are dominated by uncertainties in the HB level,  $\epsilon_V \approx 0.1$  mag. This error includes the dispersion contributed by the instantaneous magnitudes of the RR Lyrae stars. Considering in quadrature the errors of HB level and  $V$  absorption we obtain a total error in distance modulus of  $\pm 0.13$ . Accordingly, the distance from the Sun corresponds to  $d_\odot = 7.2 \pm 0.5$  kpc.

The Galactocentric coordinates of the cluster, assuming a distance of the Sun to the Galactic center of  $R_\odot = 8.0$  kpc (Reid 1993), are  $X = -1.0$  ( $X < 0$  is our side of the Galaxy),  $Y = 1.2$ , and  $Z = -0.8$  kpc. The Galactocentric distance is  $R_{GC} \approx 1.7$  kpc. We conclude that the cluster is spatially located within the bulge.

Concerning the kinematics, Harris (1996) gives a radial velocity  $v_{r,LSR} = -45$   $\text{km s}^{-1}$ . This low velocity for NGC 6642 in such central direction is compatible, within uncertainties, with the bulge rotation (Côté 1999). However, considering the distribution of globular clusters in Fig. 11 of Côté (1999), membership to the inner halo cannot be ruled out. Another possibility is that NGC 6642 is a halo cluster near perigalacticon, but in such case a higher velocity would be expected. Proper motion determination would nevertheless be necessary to rule out the halo alternative. In addition, determination of metallicity and abundance ratios would provide further constraints on the cluster membership to Galactic subsystems.

### 3.1. Variables

NGC 6642 is known to contain many variable stars. H93 reported the study of 18 RR Lyrae stars. Table 2 reports the magnitudes and colours for 11 variables from H93 and they are indicated in Fig. 4.

We confirm that V1 is not a RR Lyrae star since it is located near the tip of the giant branch. It has a too red colour and therefore it is very likely a cluster long period variable,



possibly Mira type for which Hoffleit (1972) gives  $P=216$  days. The interpretation of the red colour of V2 is more difficult. It is located on the RGB, with a considerably redder colour index than the RR Lyrae variable gap at  $0.60 < B - V < 0.90$ . However both its V magnitude (16.33) and its period measured by H93 ( $P=0.436$  days) are compatible with the cluster RR Lyrae. It is not easy to explain its anomalous colour with blends or with a variable star of the field. The remaining 9 variables are located in the expected cluster variable gap region from  $B - V = 0.61$  to  $0.83$  at an average magnitude of  $V = 16.43$ , as already reported in Section 3. As regards their location relative to the cluster center, V2 is quite close to the center of the cluster, located at about  $30''$  from the center. Half of the other variables we identified (V7, V13, V11, V12 and V3) are more distant. Therefore we confirm the previous H93's suggestion that these variables belong to the cluster. H93 obtained an average  $B_{RR} = 17.0$  and derived  $V = 16.3 \pm 0.2$  for the HB value, in very good agreement with our previous independent measurement of  $V_{HB} = 16.35$ . We cannot check directly the consistency of our photometry with H93's zero point because we have no common secondary standard, but there is no evidence for inconsistencies between the two photometries.

## 4. The Relative Age

### 4.1. Field decontamination

The relatively low latitude and bulge-intercepting line of sight of NGC 6642 imply that there is important field contamination, as shown by the width of the Main Sequence (MS) and turn-off (TO) (Fig. 5a). To minimize the effect of foreground and background field stars on the cluster CMDs we apply a decontamination procedure based on the number-density of stars present in the offset field. As offset field we use the North-South extension at the East edge of the CCD field, with size of  $23$  arcsec, this being the least cluster-contaminated frame zone. This region contains a large enough number of stars such as to produce a representative statistics of the field stars. Based on the spatial number-density of stars in the offset field, the decontamination algorithm estimates the number of field stars which within the  $1\sigma$  Poisson fluctuation should be present in the cluster field. The observed CMD is then divided into colour/magnitude cells from which stars are randomly subtracted in a number consistent with that expected for field stars in each cell. The dimensions of the colour/magnitude cells can be subsequently changed so that the total number of stars subtracted throughout the whole cluster area matches the expected one, within the  $1\sigma$  Poisson fluctuation. Since the field stars are taken from an outer region of fixed dimensions, corrections are made for the different solid angles of cluster and offset fields. This procedure was previously used in the analysis of low-contrast open clusters in the third quadrant (Bica & Bonatto 2005).

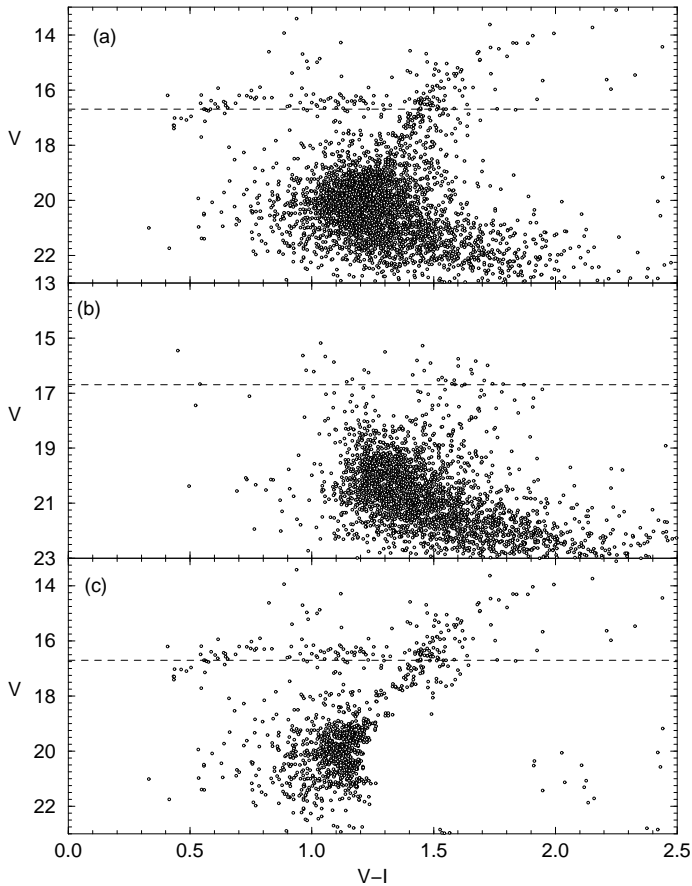


**Fig. 5.** (a) - Original  $V$  vs.  $V - I$  CMD of the central region ( $0.0 - 1.5'$ ) of NGC 6642. (b) - Same area field-star CMD extracted at the East edge of the frame. (c) - Decontaminated cluster CMD (see Sect. 4.1). The dashed line shows the short/long exposure threshold.

The method is illustrated in Fig. 5 for an extraction of  $0.0' \leq R \leq 1.5'$  in  $V$  vs.  $V - I$ , where the observed (panel (a)), same area field-star (panel (b)), and decontaminated cluster CMDs (panel (c)) are shown. In all panels short and long exposures were combined. The dashed line shows the short/long exposure borderline. The giant branch and HB of NGC 6642 are essentially not affected by field stars. On the other hand, in the original CMD (panel (a)) the subgiant branch of NGC 6642 ( $V \approx 18 - 19$ ) is considerably contaminated by field stars. In the decontaminated CMD (panel (c)) the subgiant branch is defined, although apparently somewhat depleted. This might be a real feature or a decontamination artifact. A comparison with the HST CMD of the central parts of NGC 6642 (see Fig. 14 of Piotto et al. 2002) shows similar CMDs, perhaps with the presence of a small gap at the subgiant branch level. We note that the decontamination procedure was applied as well to the bright range in Fig.5. However, the field-star density for bright stars is so low compared to that of the cluster that essentially no star was subtracted.

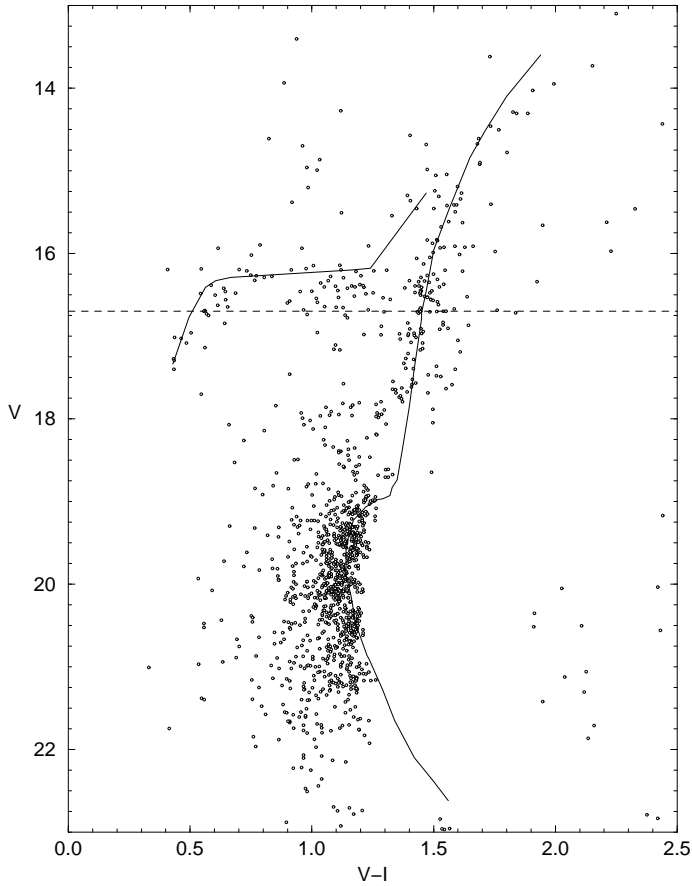


**Fig. 6.** Same as Fig.5c where the mean locus of M5 CMD is overplotted.

A fundamental result of the field subtraction (panel (c)) is the relatively narrow TO (within  $V - I \approx 1.0 - 1.2$ ), which in turn shows that bulge stars dominate the observed TO-red side (panel (a)). The decontaminated CMD helps constrain the cluster age (Sect. 4.2).

#### 4.2. Age of NGC 6642 relative to M5

Fig. 3 shows the comparison of the dereddened  $V$  vs.  $B - V$  CMD of NGC 6642 with the mean locus of the template cluster M5 (Sandquist et al. 1996). The upper sequences are very well reproduced, and by matching the blue and red parts of the HB and the GB, the M5 TO results coincident with the expected locus of NGC 6642 TO.

Fig. 6 gives the  $V$  vs.  $V - I$  decontaminated CMD with the mean locus of M5 (Johnson & Bolte 1998) overplotted, with appropriate shifts in magnitude and colour. Similarly to the BV analysis, the bright sequences are well fitted and the VI field subtracted TO is well reproduced in the range  $V - I \approx 1.0 - 1.3$ , which is considerably narrower than the distribution of stars in the BV CMD. The above indicates for NGC 6642 an age comparable to that of M5. We point out that at the RGB base some oversubtraction

seems to have occurred. However the general fit is not affected since the HB and GB extents provide constraints and leverage.

Rosenberg et al. (1999) and De Angeli et al. (2005) have shown that M 5 has an age compatible with the mean age of the halo clusters. Therefore, NGC 6642 is coeval with the halo.

## 5. Concluding Remarks

The SOAR telescope and the optical imager SOI have produced suitable scientific images of NGC 6642 in its first commissioning phase. Subarcsecond images were obtained.

A CMD reaching below the turn-off was obtained, allowing to measure its age relative to the template halo cluster M 5. NGC 6642 is coeval with M 5, and therefore with the halo.

The other parameters we obtained for NGC 6642 are consistent with the literature:  $E(B-V) = 0.42 \pm 0.03$ ,  $d_{\odot} = 7.2 \pm 0.5$  kpc, and  $[Fe/H] = -1.3$ .

It is interesting to note that this cluster shows an intermediate metallicity in the tail of the metallicity distribution of the bulge (McWilliam & Rich 1994), and that it is spatially located within the bulge volume.

It is important to note that the genuine bulge metal-poor globular clusters might be the most ancient fossil records of the Galaxy (van den Bergh 1993), and NGC 6642 may be one of these objects.

Kinematical studies, in particular proper motions, would be of great interest to verify to which component of the spheroid it belongs. A further analysis of great interest would be to derive abundance ratios from high resolution spectroscopy of individual stars, which might give hints on characteristics of inner halo or bulge population for this cluster.

*Acknowledgements.* We acknowledge the grant Instituto do Milênio - CNPq, 620053/2001-1. BB, EB and CB acknowledge partial financial support from the brazilian agencies CNPq and Fapesp. We thank Dr. Kepler de Oliveira for helpful information and the SOAR staff for carrying out the observations and pre-reducing the data. The SOAR Telescope is operated by the Association of Universities for Research in Astronomy, Inc., under a cooperative agreement between the CNPq, Brazil, the National Observatory for Optical Astronomy (NOAO), University of North Carolina, and Michigan State University, USA. SO acknowledges the Italian Ministero dell'Università e della Ricerca Scientifica e Tecnologica (MURST).

## References

- Barbuy, B., Ortolani, S., Bica, E., Desidera, S. 1999, A&A, 348, 783  
 Buonanno, R., Corsi, C.E., Fusi Pecci F. 1989, A&A, 216, 80  
 Bica, E. & Bonatto, C.J. 2005, A&A, in press (astro-ph/0508188).  
 Côté, P. 1999, AJ, 118, 406  
 Dean, J.F., Warren, P.R., Cousins, A.W.J. 1978, MNRAS, 183, 569

- De Angeli, F., Piotto, G., Cassisi, S., Busso, G., Recio-Blanco, A., Salaris, M., Aparicio, A., Rosenberg, A. 2005, astro-ph/0503594
- Harris W.E., 1996, AJ 112, 1487
- Hazen, M.L. 1993, AJ, 105, 557 (H93)
- Hoffleit, D. 1972, IBVS, no. 660
- Johnson, J.A., Bolte, M. 1998, AJ, 115, 693
- Landolt, A. 1992, AJ, 104, 340
- McWilliam, A., Rich, R.M. 1994, ApJS, 91, 749
- Minniti, D. 1995, A&A, 303, 468
- Minniti, D., Olszewski, E.W., Rieke, M. 1995, AJ, 110, 1699
- Piotto, G., King, I.R., Djorgovski, S.G. et al. 2002, A&A, 391, 945
- Recio-Blanco, A., Piotto, G., De Angeli, F., Cassisi, S., Riello, M. et al. 2005, A&A, 432, 851
- Reid, M., 1993, ARA&A 31, 345
- Rosenberg, A., Saviane, I., Piotto, G., Aparicio, A. 1999, AJ, 118, 2306
- Sandquist, E.L., Bolte, M., Stetson, P.B., Hesser, J.E. 1996, ApJ, 470, 910
- Stetson, P.B. 1994, PASP, 106, 250
- Trager S.C., King I.R., Djorgovski, S. 1995, AJ 109, 218
- van den Bergh, S. 1993, ApJ, 411, 178